

# Symbolic dynamics of biological feedback networks

Simone Pigolotti, Sandeep Krishna and Mogens H. Jensen

*Niels Bohr Institute and Niels Bohr International Academy,*

*Blegdamsvej 17, DK-2100 Copenhagen, Denmark\**

(Dated: October 27, 2018)

We formulate general rules for a coarse-graining of the dynamics, which we term ‘symbolic dynamics’, of feedback networks with monotone interactions, such as most biological modules. Networks which are more complex than simple cyclic structures can exhibit multiple different symbolic dynamics. Nevertheless, we show several examples where the symbolic dynamics is dominated by a single pattern that is very robust to changes in parameters and is consistent with the dynamics being dictated by a single feedback loop. Our analysis provides a method for extracting these dominant loops from short time series, even if they only show transient trajectories.

PACS numbers: 05.45.Ac,82.40.Bj,05.45.Tp

Many biological systems can be described by directed networks, where nodes represent different components and arrows represent interactions. In cell biology, nodes are molecules, while arrows stand for complex formation, protein modification, transcription regulation, etc. Ecosystems constitute another example, where nodes are species and arrows represent predation, competition and symbiosis. Biological functions are often performed by specific small subnetworks, or *modules* [1]. A dynamical model of a module requires, beyond the knowledge of the network structure, some hypothesis on the form of the interactions, which are often poorly characterized. It is then crucial to develop techniques to study the qualitative dynamics of modules assuming limited information.

We present a method to obtain information about patterns in the dynamics of biological feedback networks. Given the network structure, i.e., which nodes activate/repress which other nodes, it is possible to predict the ordering of maxima and minima of the dynamical variables. Vice versa, from an experimentally observed ordering one can obtain some information about the structure of the network. The method is a generalization of the one introduced in [2] for the dynamics of a single negative feedback loop, without any cross links, where a unique pattern is allowed. A More complex network structure [3, 4, 5, 6, 7, 8] allows multiple dynamical patterns. Moreover, a particular observed pattern could originate from different network structures. Nevertheless, our method can reduce the possibilities and provides non-trivial information that can guide experiments. Our technique also applies when the dynamics is transient, so that information can be obtained, for example, by watching how the concentrations of proteins and genes belonging to a given module relax to a stationary state after a perturbation. This extends the use of our formalism to cases in which oscillations are damped [7].

We consider a system described by  $N$  dynamical variables,  $x_i$ ,  $i = 1 \dots N$ , which we call “densities” and could represent, for example, the concentrations of the chemical species composing the network/module. We assume that

they evolve with time in a deterministic way, according to a system of differential equations:

$$\frac{dx_i}{dt} = g_i(x_1, x_2 \dots x_N) \quad i = 1 \dots N. \quad (1)$$

Many possible dynamical systems may correspond to a given network. The only constraints we impose are that the interactions be monotonic, i.e., each off-diagonal element of the Jacobian matrix,  $\partial_{x_j} g_i$ , is either positive everywhere in phase space (when node  $j$  activates  $i$ ), or negative everywhere ( $j$  represses  $i$ ), or zero everywhere (no arrow from  $j$  to  $i$ ). In words, activators are always activators and repressors are always repressors. Indeed, transcription factors rarely switch from being activators of a particular gene to repressors at different densities; a predator of a particular species does not become its prey when their abundances change. We do not require monotone self-interactions: a variable may activate or repress itself depending on the densities.

We associate to each state  $(x_1, x_2 \dots x_N)$  a *symbol* such as  $(+, -, -, \dots +)$ . This  $N$ -component sign vector describes which densities are increasing and which are decreasing at a given time: the  $i$ -th component is just the sign of  $g_i(x_1, x_2 \dots x_N)$ . Such a representation divides the phase space into sectors, each associated with a symbol, in which each density has a definite increasing/decreasing behavior. The sectors’ boundaries are the *nullclines*, i.e. the manifolds satisfying  $g_i(x_1, x_2 \dots x_N) = 0$ . Our goal is to determine the conditions under which the trajectory can cross a nullcline. This requires a density to change from increasing to decreasing (or vice versa) and is equivalent to determining when the density can have a maximum or minimum.

For example, a minimum for the variable  $x_i$  corresponds to a crossing of the nullcline  $g_i = 0$  from the region  $g_i < 0$  to the region  $g_i > 0$ . This is possible only if, somewhere on the nullcline, the scalar product between the vector field  $\vec{g}$  and the vector  $\nabla g_i$  (which is

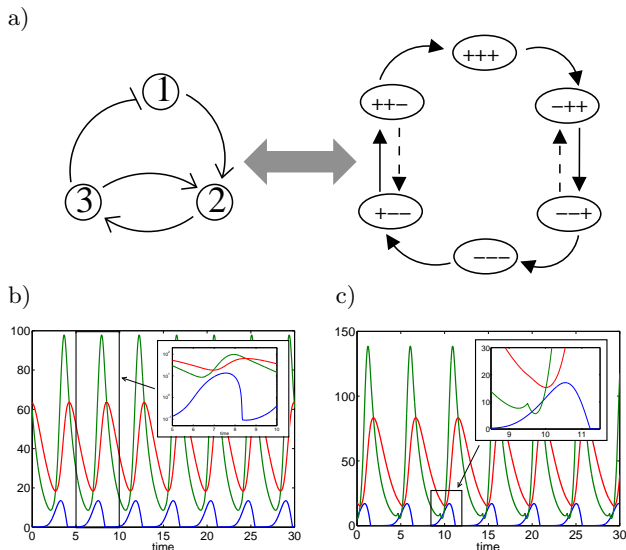


FIG. 1: Simple example of the use of symbolic dynamics. (a) (left) Scheme of the network. We represent activation by a normal arrow, and repression by a barred arrow. (right) Corresponding transition network; we removed for clarity the symbols  $(++-)$  and  $(-+-)$  which have no incoming links. (b) Dynamics of the 3 variables as a function of time with a weak cross-link ( $a = 10$ , see text), showing the transition cycle in solid arrows in (a). Inset shows the same on a log-scale. (c) Dynamics for a stronger cross-link ( $a = 50$ , see text) which includes the transitions shown by dashed arrows, zoomed in the inset. In all plots  $x_1$  is blue,  $x_2$  is green and  $x_3$  is red.

normal to the nullcline  $g_i = 0$ ) is positive:

$$\sum_{j \neq i} g_j(x_1, x_2, \dots, x_N) \partial_{x_j} g_i(x_1, x_2, \dots, x_N) > 0. \quad (2)$$

The  $i = j$  term is excluded since it is zero on the nullcline. By assumption, all the derivatives have fixed signs, and in any given sector the  $g_j$ 's also have fixed signs (encoded in the associated symbol). If the symbol and derivative signs are such that each term is negative, then the sum cannot be positive. This implies the rule: *A variable cannot have a minimum if all its repressors are increasing and all its activators are decreasing.*

Similarly, for maxima:

*A variable cannot have a maximum if all its repressors are decreasing and all its activators are increasing.*

Using the above two rules we can construct a network of allowed transitions for a given biological module, with one node for each symbol and an arrow for each transition that does not violate the above rules. Note that the transition network will only have arrows connecting symbols differing by a single sign, because each maximum or minimum corresponds to a single sign flip.

We first consider the example network of Fig. 1a(left): a three-species negative feedback loop with a cross-link from node 3 to 2 that introduces a positive feedback. By checking all the allowed transitions we construct the cor-

responding transition network, shown in Fig. 1a(right). For example, from the symbol  $(-++)$  the transition  $(-++) \rightarrow (-+-)$  is ruled out because all the activators of node 3 are increasing, therefore it cannot have a maximum. Similarly we rule out all transitions from it except  $(-++) \rightarrow (- - +)$ . The result, in this case, is a simple modification of the transition network for a single negative feedback loop shown by the solid arrows in Fig. 1a(right)[2]. With the cross link present, the additionally allowed transitions are the ones shown with dashed arrows. The following dynamical system illustrates these possibilities:  $\dot{x}_1 = c - x_1 x_3 / (k_1 + x_1)$ ;  $\dot{x}_2 = x_1^2 + a [\theta(x_3 - k_2) - 1] - x_2$ ;  $\dot{x}_3 = x_2 - x_3$ . The major nonlinearity is the Heaviside step function:  $\theta(x) = 0$  for  $x < 0$ , and  $\theta(x) = 1$  for  $x > 0$ [20]. By choosing parameters such that the cross link is weak ( $c = 30, a = 10, k_1 = 0.1, k_2 = 20$ ) one obtains dynamics of Fig. 1b, which is identical to the simple 3-species loop. As the strength of the cross link is increased ( $a = 50$ ), the symbolic dynamics changes to also exhibit the dashed transitions. This is shown in Fig. 1c where variable  $x_2$  develops a new small maximum, thus changing the symbolic dynamics.

We now move on to a system that exhibits a richer range of dynamical behaviours (see Fig. 2a). It consists of two negative feedback loops, coupled via a shared species. This network has been widely studied in the ecological literature [9, 10, 11] as a model for three trophic level ecosystems: species  $x_3$  feeds on  $x_2$ , and  $x_2$  feeds on  $x_1$ . The chaotic properties of this motif have been used to interpret data from the Canadian lynx-hare cycle, showing irregular oscillations [12].

We consider first the Hastings-Powell (HP) model [10] as a dynamical system corresponding to this network:

$$\begin{aligned} \dot{x}_1 &= rx_1(1 - kx_1) - \alpha_1 x_1 x_2 / (1 + b_1 x_1) \\ \dot{x}_2 &= -d_1 x_2 + \alpha_1 x_1 x_2 / (1 + b_1 x_1) - \alpha_2 x_2 x_3 / (1 + b_2 x_2) \\ \dot{x}_3 &= -d_2 x_3 + \alpha_2 x_2 x_3 / (1 + b_2 x_2) \end{aligned} \quad (3)$$

with the following parameter choices:  $\alpha_1 = \alpha_2 = 4$ ,  $b_1 = b_2 = 3$ ,  $d_1 = .4$ ,  $d_2 = .6$ ,  $k = 1.5$ . By increasing the parameter  $r$ , a stable limit cycle undergoes a series of period doubling bifurcations, followed by the onset of chaos. A projection of the attractor on the  $x_2 - x_3$  plane is shown in Fig.(3). The chaotic trajectory looks similar to the periodic one, except for the irregular behavior of the amplitude [11]. This means that the same sequence corresponding to the periodic orbit is observed after the onset of chaos. By increasing  $r$  even more, we found a regular window with a change in the symbolic dynamics (the ‘‘kick’’, shown in red in the attractor in Fig. 3 and in the bifurcation diagram, Fig. 4a, and corresponding to the blue dashed transition in Fig. 2b). The kick is still present when, by further increasing  $r$ , the dynamics becomes chaotic again.

The conclusion is that the same symbolic dynamics observed close to the Hopf bifurcation is found in a large

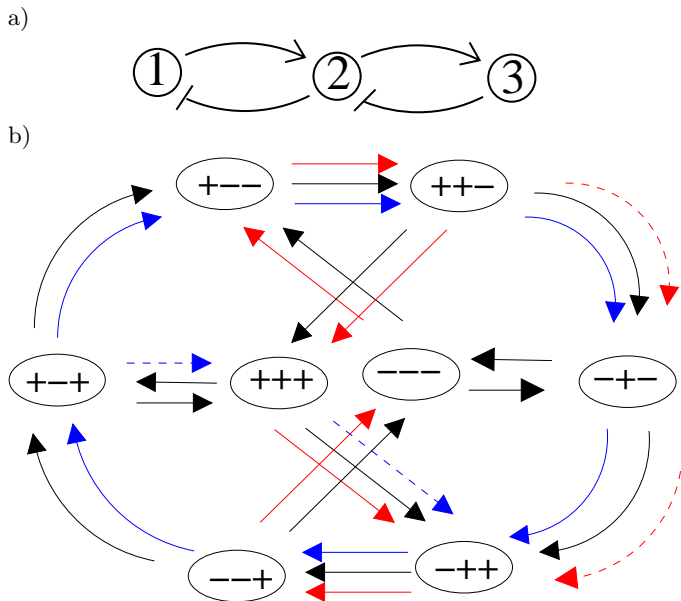


FIG. 2: Network of two coupled two-species oscillators. (a) Structure of the network. (b) The transition network for this 3-node system. Black arrows indicate all the allowed transitions. Blue arrows are the transitions actually observed in the HP system and red arrows are the transitions observed in the BHS model (see text). Dashed arrows indicate “kicks”, i.e., transitions which are *not* observed close to the Hopf bifurcation.

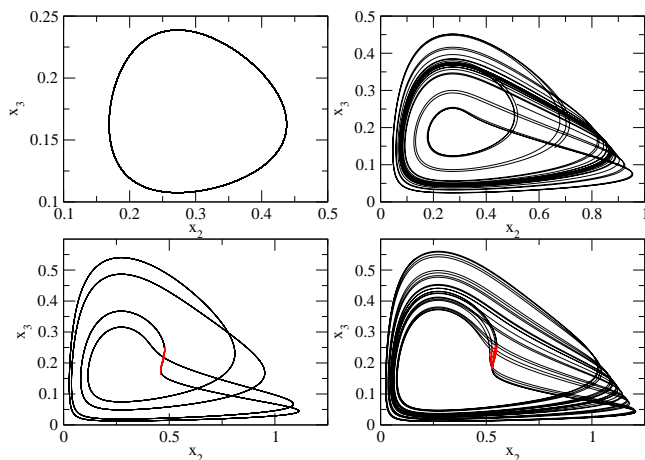


FIG. 3: Two dimensional projection of the attractor of the system of equation (3) for different values of the control parameter  $r = 2.0$  (top-left),  $r = 2.6$  (top-right),  $r = 3.0$  (bottom-left)  $r = 3.3$  (bottom-right).

region of parameter space. We compare the results with a different system corresponding to the same network, the model by Blausius, Huppert and Stone (BHS)[9]:

$$\begin{aligned}
 \dot{x}_1 &= x_1 - \alpha_1 x_1 x_2 / (1 + k x_1) \\
 \dot{x}_2 &= -d x_2 + \alpha_1 x_1 x_2 / (1 + k x_1) - \alpha_2 x_2 x_3 \\
 \dot{x}_3 &= c(x_3^* - x_3) + \alpha_2 x_2 x_3
 \end{aligned}
 \quad (4)$$

with parameters  $\alpha_1 = 2$ ,  $\alpha_2 = d = 1$ ,  $k = 0.12$ ,  $x_3^* = 0.006$ . Here, a convenient control parameter is  $c$ . We observe the same scenario in the bifurcation diagram (see Fig. (4b)): periodic orbit, then chaotic but same periodic symbolic dynamics, then different symbolic dynamics in a regular window and, finally, chaotic symbolic dynamics. Note, however, that the periodic symbolic dynamics observed close to the Hopf bifurcation is *different* from that observed in the HP model.

To test the robustness of the two sequences, we tried to change the functional form of the interaction between  $x_2$  and  $x_3$  by setting  $b_2 = 0$  in the HP model or, conversely, introducing saturated response in the BHS model. We also tried to vary the parameters of both systems, by up to 50% from their default values. The two symbolic sequences were not affected by any of these changes. A possible cause for this robust difference could be the logistic term in the first equation of (3), acting as a regulator so that the full dynamics is bottom-up controlled.

The difference between the symbolic dynamics of the HP and BHS systems can be used for model selection: in the example of the Canadian lynx system, one has access only to the lynx population time series, but temporal measurements of the hare and grass abundances could be used to understand which model is more appropriate. Interestingly, from the point of view of maxima/minima order, these two systems behave like two different, single negative feedback loops [2]:  $3 \rightarrow 2 \rightarrow 1 \rightarrow 3$  (HP system) and  $1 \rightarrow 2 \rightarrow 3 \rightarrow 1$  (BHS system). Both these “effective” loops would include an “effective” interaction between variables  $x_1$  and  $x_3$ .

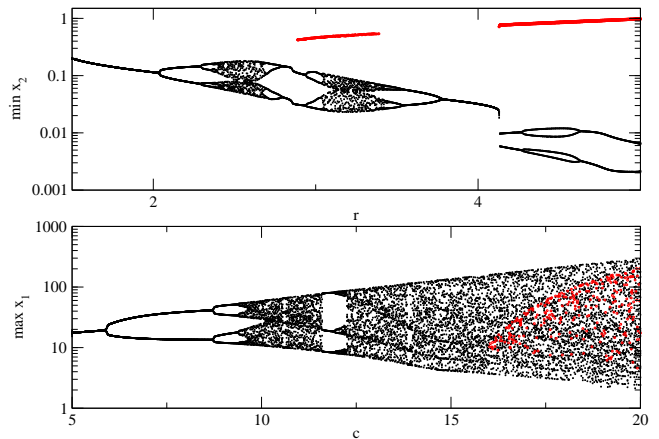


FIG. 4: Bifurcation diagrams. (top) HP model (3), minima of  $x_2$  plotted versus  $r$ . (bottom) BHS model (4), maxima of  $x_1$  versus  $c$ . In both plots, red dots indicate the appearance of “kicks” in the trajectory and symbolic dynamics (see text).

So far we have gone from a known network to the transition network to the time series. The reverse process uses the transitions observed in an experimental time series to infer information about the underlying network. For example, the circadian oscillations of the three

genes  $kaiA, B, C$  in cyanobacteria [13] were shown in ref. [2] to have the following symbolic dynamics  $(B, A, C)$ :  $(+++)$   $\rightarrow$   $(-++)$   $\rightarrow$   $(--+) \rightarrow$   $(---) \rightarrow$   $(+--)$   $\rightarrow$   $(++-)$   $\rightarrow$   $(+++)$ . Several networks are consistent with this pattern – the simplest is the loop  $B \rightarrow A \rightarrow C \rightarrow B$ , as suggested in ref. [2]. Experiments have shown that  $A \rightarrow C$  and  $C \rightarrow B$ , and that all three genes are essential for oscillations [14]. With this information we can get non-trivial guidelines for which further interactions to look for experimentally: (i)  $kaiA$  must be either activated by  $kaiB$ , or repressed by  $kaiC$  (or both), (ii) if  $kaiA$  is not activated by  $kaiB$  then, in addition to  $kaiC \rightarrow kaiA$ ,  $kaiB$  must activate  $kaiC$ , so that the underlying network looks similar to Fig. 2a. Of course, these predictions are for “effective” interactions, which at the molecular level could involve multiple intermediates, such as chemical complexes and various protein activity states. Ref. [2] shows how the method can reconstruct effective interactions even in the presence of intermediate species.

This circadian example also points out how much information our method provides. The transition  $(+++)$   $\rightarrow$   $(-++)$  means that either  $B \rightarrow A$  or  $C \rightarrow A$ . Later transitions show that either  $A \rightarrow B$  or  $C \rightarrow B$ , and  $A \rightarrow C$  or  $B \rightarrow C$ . Even without the extra experimental information, our method reduces the possibilities for the adjacency matrix of the underlying network from  $3^6$  to  $5^3$ , a factor of  $\approx 6$ . In a general  $N$  node system, with  $M$  independent observed transitions, the fraction of allowed adjacency matrices is  $[1 - (2/3)^{N-1}]^M$ ; the smaller the network and the more the transitions seen, the more useful the method. A full oscillation cycle would show at least  $N$  independent transitions. If the system instead reaches a fixed point, the transient can still be used.

Our method can be considered as complementary to the “threshold method”, described in Refs. [15, 16, 17, 18], which provides a different way of dividing the phase space into sectors, based on a choice of thresholds for each variable. The “threshold” method generates a transition diagram, which depends on parameter values. It is particularly suited to cases where the input functions are Boolean or step-like, so thresholds can be easily identified, and self-interactions are piecewise linear [19]. Our “derivative” method, in contrast, requires no choice of thresholds, generates a diagram independent of parameter values, and works for arbitrary self-interactions, but requires monotonicity in the other interactions.

In summary, we showed a method to construct a symbolic transition network that imposes a strong constraint on the dynamics monotone systems, like many biological modules. In all the cases we studied, the periodic sym-

bolic dynamics observed close to the Hopf bifurcation is found in a large region of parameter space, even when the system becomes chaotic. This explains the commonly observed phenomenology of a chaotic attractor consisting of oscillations with randomly varying amplitude [11]. The oscillatory systems we looked at produce a symbolic sequence identical to that of a single negative feedback loop for most studied parameter values. By identifying these loops, our method can be used to derive minimal models of complex, oscillatory biological systems.

We acknowledge Leon Glass for stimulating discussions and the Danish National Research Foundation and VIL-LUM KANN RASMUSSEN Foundation for funding.

---

\* URL: <http://cmol.nbi.dk>

- [1] L. H. Hartwell, J. J. Hopfield, S. Leibler and A. W. Murray, *Nature* **402**, 676 (1999).
- [2] S. Pigolotti, S. Krishna, M. H. Jensen, *Proc. Natl. Acad. Sci.* **104**16, pp. 6533-6537 (2007).
- [3] J. Mallet-Paret, J and H. L. Smith, *J Dyn Diff Equations* **2**, 367-421 (1990).
- [4] J. Bechhoefer, *Rev. Mod. Phys.* **77**, pp. 783-836 (2005).
- [5] D. A. Rand, B. V. Shulgin, J. D. Salazar and A. J. Millar, *Jour. Theo. Biol.*, **238**(3) pp. 616-635 (2006).
- [6] M. Kaufman, C. Soulé and T. Thomas, *Jour. Theo. Bio.* **248**, 675-685 (2007).
- [7] G. Tiana, S. Krishna, S. Pigolotti, M.H. Jensen, and K. Sneppen, *Phys. Biol.* **4**, R1-R17, (2007).
- [8] J. Ross, *J. Phys. Chem. A* **112**, 2134-2143 (2008).
- [9] B. Blasius, A. Huppert, L. Stone, *Nature* **399**, pp. 354-359 (1999).
- [10] A. Hastings, T. Powell, *Ecology* **72**(3), pp. 896-903 (1991).
- [11] L. Stone, D. He, *Jour. Theo. Bio.* **248** 382-390 (2007).
- [12] J. Gamarra and R. Solé, *Ecol. Lett.* **3**, pp. 114-121 (2000).
- [13] K. Kucho, K. Okamoto, Y. Tsuchiya, et al., *J. Bacteriol.* **187**, 2190–2199 (2005).
- [14] M. Ishiura, S. Katsuna, S. Aoki, et al., *Science* **281**, 1519–1523, (1998).
- [15] T. J. Perkins, M. T. Hallett, L. Glass. *J. Theor. Biol.* **230**, 289299 (2004).
- [16] T. J. Perkins, J. Jaeger, J. Reinitz, L. Glass. *PLoS Comput. Biol.* **2** e51 (2006).
- [17] L. Glass, S.A. Kaufmann, *Jour. Theo. Bio.***39**(1), 103–129 (1973).
- [18] L. Glass, *Jour. Chem. Phys.* **63**(4), 1325–1335 (1975).
- [19] E. Plahte and S. Kjoglum, *Physica D* **201**, 150-176 (2005).
- [20] We can safely introduce a discontinuous field because our argument works as long as trajectories are continuous.